

When does colonisation of a semi-arid hillslope generate vegetation patterns?

Jonathan A. Sherratt

Journal of Mathematical Biology

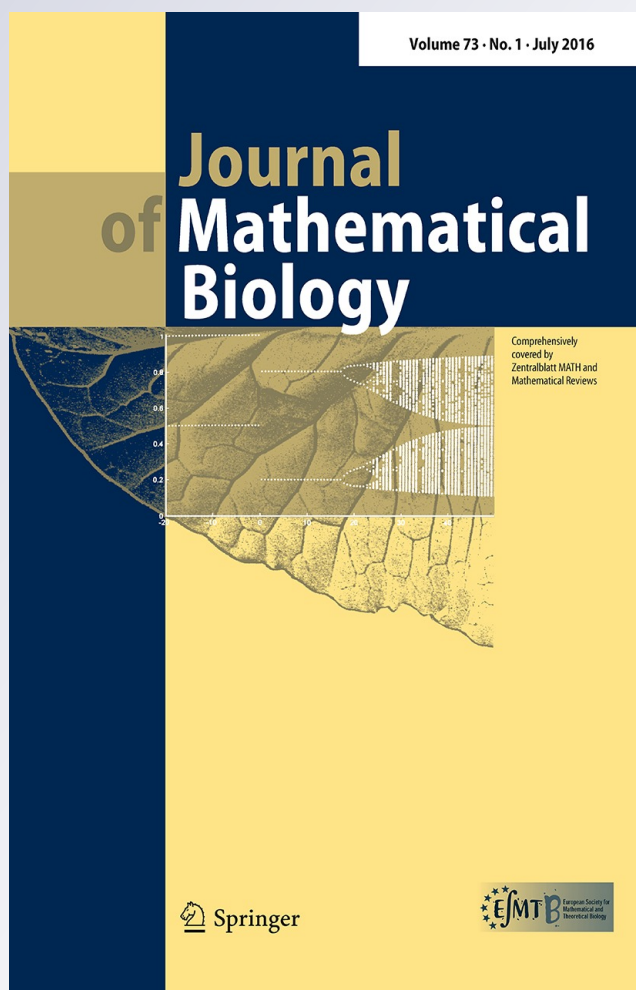
ISSN 0303-6812

Volume 73

Number 1

J. Math. Biol. (2016) 73:199-226

DOI 10.1007/s00285-015-0942-8



Your article is protected by copyright and all rights are held exclusively by Springer-Verlag Berlin Heidelberg. This e-offprint is for personal use only and shall not be self-archived in electronic repositories. If you wish to self-archive your article, please use the accepted manuscript version for posting on your own website. You may further deposit the accepted manuscript version in any repository, provided it is only made publicly available 12 months after official publication or later and provided acknowledgement is given to the original source of publication and a link is inserted to the published article on Springer's website. The link must be accompanied by the following text: "The final publication is available at link.springer.com".



When does colonisation of a semi-arid hillslope generate vegetation patterns?

Jonathan A. Sherratt¹

Received: 26 March 2015 / Revised: 5 September 2015 / Published online: 7 November 2015
© Springer-Verlag Berlin Heidelberg 2015

Abstract Patterned vegetation occurs in many semi-arid regions of the world. Most previous studies have assumed that patterns form from a starting point of uniform vegetation, for example as a response to a decrease in mean annual rainfall. However an alternative possibility is that patterns are generated when bare ground is colonised. This paper investigates the conditions under which colonisation leads to patterning on sloping ground. The slope gradient plays an important role because of the downhill flow of rainwater. One long-established consequence of this is that patterns are organised into stripes running parallel to the contours; such patterns are known as banded vegetation or tiger bush. This paper shows that the slope also has an important effect on colonisation, since the uphill and downhill edges of an isolated vegetation patch have different dynamics. For the much-used Klausmeier model for semi-arid vegetation, the author shows that without a term representing water diffusion, colonisation always generates uniform vegetation rather than a pattern. However the combination of a sufficiently large water diffusion term and a sufficiently low slope gradient does lead to colonisation-induced patterning. The author goes on to consider colonisation in the Rietkerk model, which is also in widespread use: the same conclusions apply for this model provided that a small threshold is imposed on vegetation biomass, below which plant growth is set to zero. Since the two models are quite different mathematically, this suggests that the predictions are a consequence of the basic underlying assumption of water redistribution as the pattern generation mechanism.

Keywords Semi-arid · Pattern formation · Desert · Colonization · Reaction–diffusion–advection · Periodic travelling wave

✉ Jonathan A. Sherratt
J.A.Sherratt@hw.ac.uk

¹ Department of Mathematics and Maxwell Institute for Mathematical Sciences,
Heriot-Watt University, Edinburgh EH14 4AS, UK

Mathematics Subject Classification 92D40 · 35M30 · 35C07

1 Introduction

Patterned vegetation occurs in many semi-arid regions of the world, including Africa (Deblauwe et al. 2012; Müller 2013), Australia (Berg and Dunkerley 2004; Moreno-de las Heras et al. 2012), North America (Pelletier et al. 2012; Penny et al. 2013), the Middle East (Buis et al. 2009; Sheffer et al. 2013), and Asia (Yizhaq et al. 2014). Such patterns consist of vegetated regions separated by bare ground. They are usually labyrinthine or spotted on flat terrain, but on slopes the typical form is stripes running parallel to the contours, known as “banded vegetation” or “tiger bush” (Deblauwe et al. 2008, 2011; Meron 2012). Most authors attribute pattern formation to positive feedback between vegetation and water availability. The infiltration rate of rainwater into bare semi-arid soils is very low, but it increases significantly with vegetation density (Rietkerk et al. 2000; Thompson et al. 2010), due to increasing levels of organic matter in the soil, and to the presence of root networks (Galle et al. 1999; Archer et al. 2012). This results in greater water availability, and thus increased plant growth, when vegetation biomass is larger. This positive feedback loop is known as the “water redistribution hypothesis” for vegetation pattern formation (Thompson et al. 2011; Pueyo et al. 2013).

In addition to their intrinsic fascination as an example of ecosystem-scale self-organisation, vegetation patterns are important as potential early warning signals of climate change and imminent regime shifts (Rietkerk et al. 2004; Kéfi et al. 2007; Corrado et al. 2014). Therefore they have been the subject of intensive study over the last decade. There are no laboratory replicates of vegetation patterns, and field experiments are difficult and expensive—as well as being of limited utility given the long space and time scales involved in the pattern formation process. Therefore mathematical models play a key role in understanding these ecosystems, and many different models have been proposed. The majority of these are based on the water redistribution hypothesis discussed above, with the models of Klausmeier (1999), Rietkerk et al. (2002), von Hardenberg et al. (2001) and Gilad et al. (2004, 2007) being in particularly widespread use. However it is important to comment that models have also been used to investigate alternative pattern formation mechanisms (Lefever and Lejeune 1997; Lefever et al. 2009; Pelletier et al. 2012; Martínez-García et al. 2014).

Almost all modelling studies have assumed that patterns form from a starting point of uniform vegetation, for example as a response to a decrease in mean annual rainfall (Fig. 1). Many authors additionally investigate the subsequent transitions between different patterned states as environmental conditions such as rainfall are varied (e.g. Meron 2012; Gowda et al. 2014). However there is an alternative possibility, that a pattern forms when bare ground is colonised. This has the potential to give very different relationships between pattern properties and environmental variables, and in fact I have recently shown that for banded vegetation, colonisation of bare ground and degradation of uniform vegetation give opposite trends in the relationship between pattern wavelength and slope (Sherratt 2015). To my knowledge Bel et al. (2012) are the only other authors to have modelled pattern formation via colonisation. Using

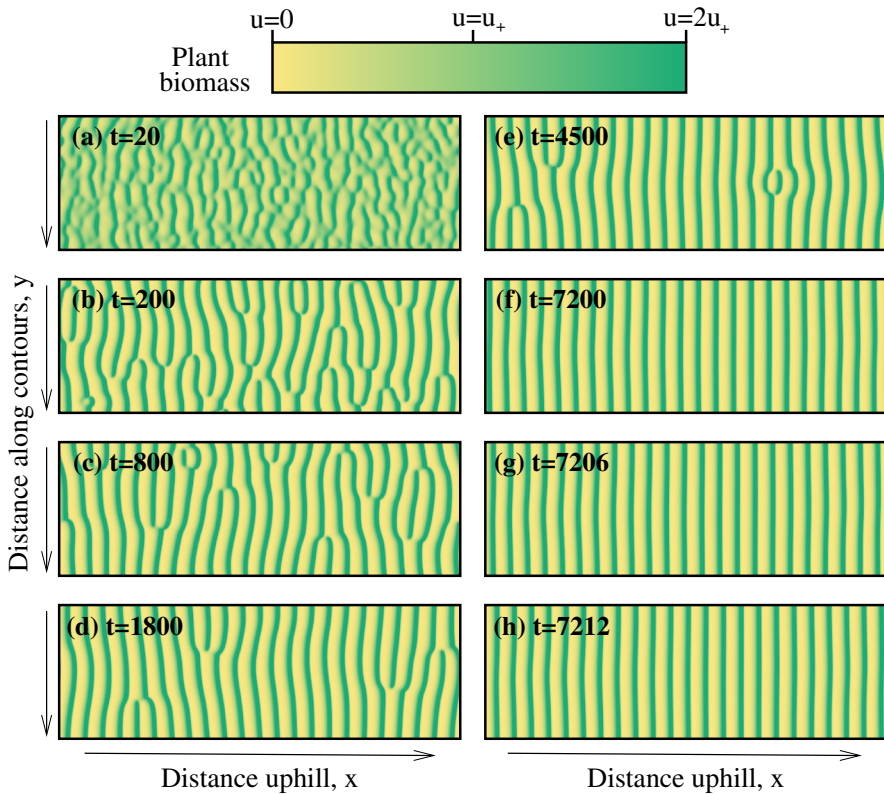


Fig. 1 A simulation of (1) showing the formation of a banded vegetation pattern from a starting point of uniform vegetation. The shading indicates plant biomass, as shown in the scalebar. At time $t = 0$ I impose a small random perturbation to the uniformly vegetated steady state (u_+, w_+) . A spatial pattern develops, which ultimately evolves to a one-dimensional pattern of stripes of running parallel to the contours. The times in **f–h** are chosen to illustrate the gradual uphill migration of the stripes. The spatial domain is $0 < x < 450$ and $0 < y < 150$ with periodic boundary conditions. For the initial conditions ($t = 0$), I applied a random perturbation of $\pm 5\%$ at each node of a grid with spacing 5, and calculated intermediate initial values using bilinear interpolation. The equations were solved using an alternating direction implicit finite difference method with upwinding, with a uniform grid spacing of 0.5 and a time step of 0.00125

a “minimal model” for vegetation dynamics in semi-arid environments, Bel et al. investigate the formation and spread of isolated regions of patterned vegetation within an unvegetated background state, on flat terrain. This last assumption is important because slope can have a major effect on processes governed by water redistribution, due to the downhill flow of water both on the surface and within the soil (e.g. Deblauwe et al. 2012; Dralle et al. 2014).

In this paper I study colonisation of sloping bare ground. My objective is to determine the conditions under which this will generate vegetation patterns—which will be stripes (bands) because of the organising effect of the slope. In Sect. 2 I introduce the Klausmeier (1999) model that forms the basis of most of my study, and I discuss my overall methodology. In Sect. 3 I consider colonisation in a basic version of the model, showing that colonisation never generates patterned vegetation. In Sect. 4 I show that,

by contrast, patterning via colonisation is predicted in an “extended” version of the model in which a diffusion term is included in the equation for water. In Sect. 5 I describe the [Rietkerk et al. \(2002\)](#) model, which is a widely used alternative model, and I show that this makes the same predictions provided that a small amendment is made to the model equations; I will argue that this amendment improves the realism of the model. I conclude by considering the ecological realism of the parameter ranges in which colonisation generates patterns, and I discuss the (limited) field data on the historical origin of vegetation patterns.

2 A simple mathematical model

Mathematical models for vegetation patterning vary from minimal (“toy”) models ([Bel et al. 2012](#)) to detailed multi-scale representations of soil-water dynamics ([Stewart et al. 2014](#)). I will attempt to survey behaviour across parameter space, which poses a major restriction on model complexity. Therefore I will focus attention on the [Klausmeier \(1999\)](#) model. This is one of the earliest and simplest models for vegetation patterning, and when suitably nondimensionalised ([Klausmeier 1999](#); [Sherratt 2005](#)) the model equations are:

$$\begin{aligned}
 \partial u / \partial t &= \overbrace{wu^2}^{\text{plant growth}} - \overbrace{Bu}^{\text{plant loss}} + \overbrace{\partial^2 u / \partial x^2 + \partial^2 u / \partial y^2}^{\text{plant dispersal}} \\
 \partial w / \partial t &= \underbrace{A}_{\text{average rainfall}} - \underbrace{w}_{\text{evaporation \& drainage}} - \underbrace{wu^2}_{\text{uptake by plants}} + \underbrace{v \partial w / \partial x}_{\text{flow downhill}} + \underbrace{D(\partial^2 w / \partial x^2 + \partial^2 w / \partial y^2)}_{\text{diffusion of water}}.
 \end{aligned}
 \tag{1}$$

Here u and w denote plant biomass and water density respectively; they are functions of time t and the distances x in the uphill direction and y parallel to the contours. For simplicity I restrict attention to uniformly sloping terrain.

The key assumption in (1) is that the per capita rate of water uptake is proportional to plant biomass, reflecting the positive correlation between infiltration rate and biomass that was discussed in Sect. 1. Plant growth rate is assumed to be proportional to water uptake on the basis that water is the limiting resource; however it should be noted that in some semi-arid regions nitrogen availability can also limit plant growth ([Hooper and Johnson 1999](#); [Stewart et al. 2014](#)). Plant loss is assumed to have a simple linear form. Some recent models have included soil toxicity, which can arise via the decay of dead plant material, showing that this can play a significant role in vegetation pattern formation ([Cartení et al. 2012](#); [Marasco et al. 2014](#)); however this is excluded from (1). Plant dispersal is represented by linear diffusion: this simplification is made for mathematical convenience, and some subsequent models use a more realistic nonlocal dispersal term ([Pueyo et al. 2008](#); [Baudena and Rietkerk 2013](#)). The (dimensionless) parameter A is proportional to mean annual rainfall. The use of a constant rainfall rate is a major simplification, since in most semi-arid regions rainfall occurs principally at certain times of year, and then only in relatively brief storms ([Istanbulluoglu and](#)

Bras 2006; Caylor et al. 2014). Both of these complications have been considered in previous modelling studies (Ursino and Contarini 2006; Guttal and Jayaprakash 2007; Vezzoli et al. 2008; Kletter et al. 2009; Siteur et al. 2014a). The parameter B reflects both natural plant loss and the effects of herbivory. As well as grazing by wild and domestic animals, “herbivory” of woody vegetation includes human removal of trees for fuel, which has a significant effect on vegetation dynamics in many semi-arid regions (Berg and Dunkerley 2004; Dembélé et al. 2006; Hejmanová et al. 2010). The parameter ν measures slope gradient. Some more recent models use representations of downhill water flow that are more detailed than the simple advection term in (1); in particular Gilad et al. (2004, footnote 18) derive a representation of surface water flow using shallow water theory. The final parameter D is the water diffusion coefficient; Ursino (2005) showed that a diffusion term always accompanies the advection term when water transport is derived from the Richards equation for soil water flow. More detailed representations of water flow in the context of modelling vegetation patterns are considered by von Hardenberg et al. (2001) and Meron et al. (2004). A final simplification made in (1) is that all of the parameters are homogeneous in space. I will retain this assumption throughout this paper, but it should be noted that recent research has highlighted the potential importance of parameter heterogeneity in models for semi-arid vegetation, in particular its ability to increase resilience to reductions in rainfall (Yizhaq et al. 2014; Bonachela et al. 2015).

Despite these various caveats, Eq. (1) remains a highly influential model that is in widespread use in both simulation-based research (Sherratt and Lord 2007; Liu et al. 2008; Borthagaray et al. 2010; Ursino and Contarini 2006; Zelnik et al. 2013; Sherratt 2013a; Siteur et al. 2014b) and analytical studies (Sherratt 2010, 2011, 2013b, c, d; Kealy and Wollkind 2012; van der Stelt et al. 2013; Siero et al. 2015). In Sect. 5 I will present a briefer and less comprehensive study of colonisation in the alternative Rietkerk model (HilleRisLambers et al. 2001; Rietkerk et al. 2002).

There are either one or three spatially homogeneous steady state solutions of the model (1). The “desert” steady state $(0, A)$ is always locally stable, and for $A \geq 2B$ there are also

$$(u_{\pm}, w_{\pm}) = ([A \pm \sqrt{A^2 - 4B^2}]/2B, [A \mp \sqrt{A^2 - 4B^2}]/2).$$

(u_-, w_-) is always unstable, while (u_+, w_+) is locally stable to spatially homogeneous perturbations provided that $B < 2$. For larger B (1) can have oscillatory dynamics which are never observed in reality; however all ecologically based parameter estimates give $B < 2$ (Klausmeier 1999; Ursino 2005) and I will assume this restriction throughout this paper. For some parameters (u_+, w_+) is unstable to inhomogeneous perturbations, and spatial patterns then occur (Fig. 1). They consist of peaks and troughs of plant biomass u , which correspond to the vegetation bands and bare interbands seen in the field.

The destabilisation of (u_+, w_+) occurs via a Turing–Hopf bifurcation, meaning that when the real part of the temporal eigenvalue changes sign, there is a non-zero imaginary part (Sherratt 2005; van der Stelt et al. 2013). This is a standard feature of models with directional transport (Anderson et al. 2012). It follows that the patterns are not stationary, and they move in the positive x direction (uphill) (Fig. 1d–f). The

issue of uphill migration of vegetation has traditionally been contentious, because of contradictory reports from early field studies (Worrall 1959; White 1969). Complicating factors in assessing migration include its very slow speed [$< 1 \text{ m year}^{-1}$ (Valentin et al. 1999, Table 5)] and the temporary expansions and contractions of the vegetation bands in response to fluctuations in environmental variables such as rainfall (Tongway and Ludwig 2001). However in recent years,¹ detailed comparisons have become possible between modern satellite images and declassified spy satellite images from the 1960s. This suggests that some banded vegetation patterns are stationary, but provides clear evidence of uphill migration in other cases, with a typical time taken to move one wavelength being about 100 years (Deblauwe et al. 2012). The biological basis for migration of vegetation bands is that the upslope edge of the bands is wetter than the downslope edge, resulting in higher seedling densities and lower levels of plant death; these differences are observed in the field (Wu et al. 2000; Tongway and Ludwig 2001). The observation of stationary patterns on sloping terrain is not consistent with (1) and their occurrence has been attributed to various factors excluded from the model, including compaction of unvegetated soil (Dunkerley and Brown 2002) and preferential dispersal of seeds in the downhill direction, due to transport in run-off (Saco et al. 2007; Thompson and Katul 2009).

An important precursor to the study of pattern generation via colonisation is to consider the parameter region in which patterns exist. In applications one is primarily interested in the effects of varying rainfall, and so I will focus on the values of the parameter A giving patterns. I denote by A_{TH} the pattern onset (Turing–Hopf bifurcation) point. Analytical calculation of A_{TH} seems impossible when $\nu \neq 0$, but a leading order expression for large ν when $D = 0$ is given in (Sherratt 2013c). Since this is a bifurcation of the uniformly vegetated state (u_+, w_+) , A_{TH} is necessarily greater than $2B$ which is the threshold value of A below which this uniform state does not exist. However patterns themselves do exist for $A < 2B$ (Sherratt 2013a, c, d; Siteur et al. 2014b), with the minimum rainfall for patterns being given by another critical point $A_{min} < 2B$. Again, an analytical formula for A_{min} is not available, but a leading order expression for large ν and $D = 0$ has been calculated (Sherratt 2013d). Intuitively, for $A < A_{min}$ there is insufficient rainfall to support vegetation; for $A_{min} < A < A_{TH}$ vegetation is viable but only in the context of patterns; and for $A > A_{TH}$ there is enough rainfall to maintain uniform vegetation. The fact that $A_{min} < 2B$ reflects the ability of vegetation to survive in patterns at rainfall levels for which uniform vegetation is not viable.

Klausmeier's original paper (Klausmeier 1999) did not include a water diffusion term, although this has been added by a number of subsequent authors (Ursino 2005; Kealy and Wollkind 2012; Zelnik et al. 2013; Siteur et al. 2014b). Therefore (1) is often known as the “modified” or “extended” Klausmeier model. I will begin my investigation of the potential for colonisation to generate patterns using the original form of the model, that is with $D = 0$. In Sect. 4 I will then investigate the way in which my results are altered by the inclusion of water diffusion.

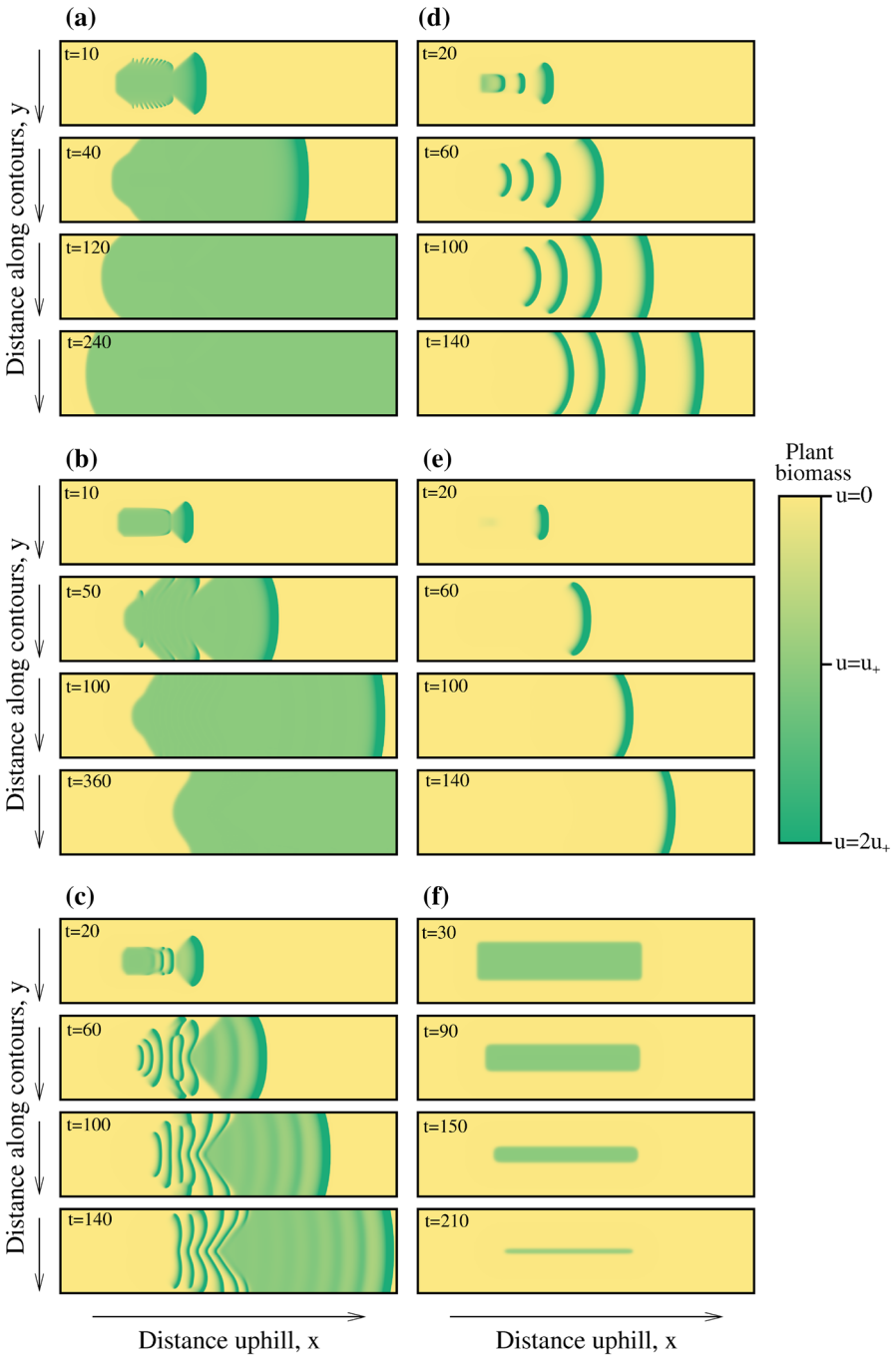
¹ Assessment of vegetation band migration using satellite imagery was made possible by the declassification in 1995 of images from the US satellite missions Corona (1959–1972), Argon (1961–1964) and Lanyard (1963).

3 Colonisation with no water diffusion

In this section I will show that in the absence of water diffusion ($D = 0$) colonisation of a bare hillslope always generates uniform vegetation rather than a pattern. I use the term “colonisation” to refer to the establishment of vegetation from a localised vegetated region in otherwise bare ground. My calculations in this section act as ground work for a consideration of the more general situation ($D \neq 0$) and it is important to emphasise that they do not imply that colonisation cannot generate patterns in real ecosystems. This is because Klausmeier’s (1999) original exclusion of water diffusion is unrealistic. Klausmeier included the water advection term in his model on phenomenological grounds. Subsequently Ursino (2005) showed that the term can be derived from the Richards equation for soil water flow, but only in conjunction with a diffusion term. Moreover, water diffusion corrects a major shortcoming of the model predictions: when $D = 0$, Eq. (1) predicts that patterns will not form on flat ground. This is at odds with the frequent occurrence of labyrinthine or spotted patterns on flat ground in the field (Deblauwe et al. 2008, 2011). In his original paper Klausmeier (1999) suggested that such patterns might mirror small scale variations in topography, but subsequent detailed investigation showed that this is not the case (Barbier et al. 2006). The addition of water diffusion rectifies the situation, since patterns can form when $v = 0$ (flat ground) provided that D is sufficiently large. This was first demonstrated by Kealy and Wollkind (2012), and the generalised model framework (1) has been adopted in a number of recent studies (Zelnik et al. 2013; Siteur et al. 2014b; Sherratt 2015; Siero et al. 2015).

Figure 2 shows model simulations of vegetation dynamics on a uniform hillslope for various values of the rainfall parameter A . These simulations illustrate that when the rainfall is high enough to enable colonisation, the resulting vegetation is uniform rather than patterned; later in this section I will present a detailed study showing that this is a general result, applying for all parameter values (when $D = 0$). In the simulations I impose a localised region of vegetation onto bare ground, and monitor the subsequent dynamics. As one expects intuitively, when rainfall A is sufficiently large, the initial patch of vegetation expands in both directions, so that the hillside is colonised (Fig. 2a). At lower rainfall levels, the initial patch expands along the contours and in the uphill direction, but the downslope edge also moves uphill (Fig. 2b–e). This is because the downhill flow of water causes the upslope edge of the vegetated region to be wetter than the downslope edge. Consequently plant loss is less than growth rate at the upslope edge, and greater than growth rate at the downslope edge. This is the same process that leads to uphill migration of banded vegetation patterns (discussed in Sect. 2). In both of Fig. 2a, b the vegetation between the two edges of the patch remains uniform. However at lower rainfall levels a pattern forms (Fig. 2c, d); note that this only occurs when the upslope and downslope edges both move uphill so that there is no colonisation. At even lower rainfall levels the initial patch of vegetation either migrates uphill (Fig. 2e) or simply collapses (Fig. 2f).

The results shown in Fig. 2 are typical across a wide range of parameter values. The key to understanding them in detail lies in an investigation of interfaces between uniform vegetation and bare ground, in one space dimension (no y dependence). I will calculate threshold values of A for such interfaces to move in the uphill or downhill



◀ **Fig. 2** The dynamics of a localised patch of vegetation on a uniform hillslope, as predicted by the model (1) when the water diffusion coefficient $D = 0$. Colonisation occurs in **a** since the upslope and downslope edges of the vegetation patch move in the uphill and downhill directions respectively. In **b–e** there is no colonisation because both the upslope and downslope edges move in the uphill direction, while in **f** the initial vegetation patch simply collapses. The plotted region is $0 < x < 600, 0 < y < 150$. In **a–e** I set $u(x, y, t = 0) = u_+$ when $100 < x < 200$ and $60 < y < 90$ with $u(x, y, t = 0) = 0$ otherwise; $w(x, y, t = 0) \equiv A$. In **f** the initial vegetation patch is larger to give greater visual clarity: $100 < x < 400$ and $37.5 < y < 112.5$. The values of the rainfall parameter A and the slope parameter ν are indicated above the plots; the plant loss parameter $B = 0.45$ in all cases. The shading indicates vegetation density, as shown in the scalarbar. In **c–f** I solve the equations on the plotted region, but in **a** and **b** the solution domain extends to $x = 1800$ (though only $0 < x < 600$ is plotted) in order that vegetation does not invade to the right hand boundary. In all cases the boundary conditions are periodic in y and Dirichlet ($u = 0, w = A$) at $x = 0$ and at **a, b** $x = 1800$ or **c–f** $x = 600$. These Dirichlet boundary conditions are appropriate because the time intervals over which I run the simulations are in all cases short enough that vegetation does not spread to either boundary. I use a different value of ν in **f** in order to give a parameter set that lies in region I of Fig. 6. The equations were solved using an alternating direction implicit finite difference method with upwinding, with a uniform grid spacing of 0.2 and a time step of **a–e** 0.0036, **f** 0.02. These give a CFL number of **a–e** 0.8, **f** 0.05

directions, and by comparing these thresholds with the Turing–Hopf point A_{TH} I will show that colonisation never generates patterns (when $D = 0$). I begin by considering interfaces with the bare ground state $(0, A)$ on the downhill side ($x \rightarrow -\infty$) and the uniformly vegetated state (u_+, w_+) on the uphill side ($x \rightarrow +\infty$), as illustrated schematically in Fig. 3a. In numerical simulations (not illustrated for brevity), such interfaces evolve to travelling wave fronts whose velocity decreases as rainfall A increases. When rainfall is low the velocity is positive, meaning that the bare ground region expands and the vegetated region contracts; correspondingly when rainfall is high the velocity is negative and the bare ground region contracts while the vegetated region expands. I denote by $A_{crit,1}$ the critical value of the rainfall parameter at which the velocity is zero; in physics terminology $A_{crit,1}$ is a Maxwell point. This behaviour is entirely expected intuitively: an increase in rainfall promotes vegetation spread. Although I am not aware of mathematical theorems that can be applied to this type of front dynamics for (1), the behaviour is also exactly as one would expect mathematically. Since $(0, A)$ and (u_+, w_+) are both locally stable one expects evolution to a wave front whose speed is uniquely determined by the model parameters. Moreover a straightforward phase plane calculation shows that as A increases the basin of attraction of $(0, A)$ in the local dynamics decreases, while that of (u_+, w_+) increases, so that one expects the wave velocity to decrease. This behaviour is entirely reminiscent of front dynamics in simple bistable systems such as the Fitzhugh–Nagumo equation (Murray 2003).

At $A = A_{crit,1}$ there is a stationary transition front, satisfying

$$\partial^2 u / \partial x^2 + wu^2 - Bu = 0 \tag{2a}$$

$$\nu \partial w / \partial x + A - wu^2 - w = 0 \tag{2b}$$

with $(u, w) \rightarrow (0, A)$ as $x \rightarrow -\infty$ and $(u, w) \rightarrow (u_+, w_+)$ as $x \rightarrow +\infty$. At $(0, A)$ the eigenvalues of (2a) can be calculated immediately as ν and $\pm B^{1/2}$. At (u_+, w_+) the eigenvalues λ satisfy

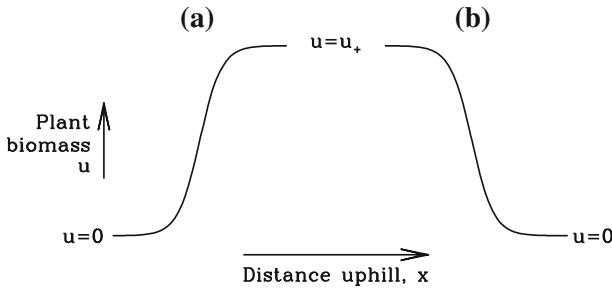


Fig. 3 A schematic illustration of the two types of interface considered in Sect. 3. In **a** there is uniform vegetation on the uphill side and bare ground on the downhill side; the reverse applies in **b**

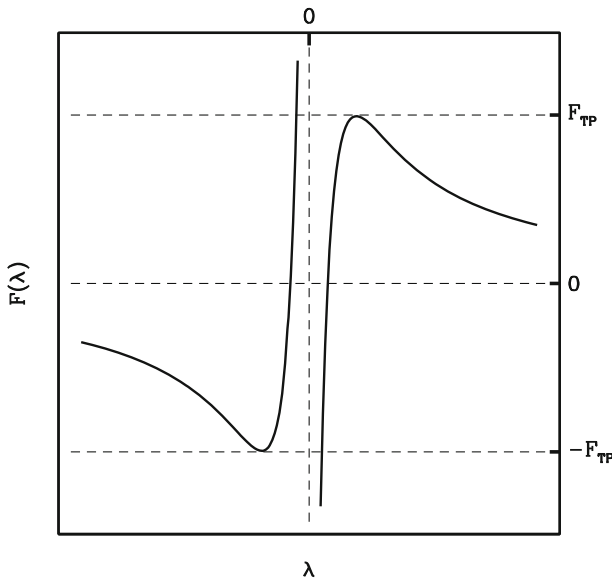


Fig. 4 The qualitative form of the function $F(\cdot)$, defined in (3)

$$v = F(\lambda) \equiv \frac{\lambda^3 + B\lambda}{(1 + u_+^2)\lambda^2 - B(u_+^2 - 1)}. \tag{3}$$

Since $u_+ > 1$, $F(\cdot)$ has the qualitative form shown in Fig. 4: note that it is an odd function of λ , and differentiation shows immediately that there are only two finite turning points, at which $F = \pm F_{TP}$ say. Therefore when $v < F_{TP}$ there are three real eigenvalues, two positive and one negative, while for $v > F_{TP}$ there is one real negative eigenvalue and a complex conjugate pair of eigenvalues. The latter have positive real part for v just above F_{TP} . Suppose now that the real part was negative for larger values of v . Then there would be a value of v for which there was a real negative eigenvalue and two pure imaginary eigenvalues; the product of these would be positive, which contradicts (3). Therefore for all $v > F_{TP}$ there is one real negative eigenvalue and a complex conjugate pair of eigenvalues with positive real part. It follows that for all

v the transition front solution of (2a) must approach (u_+, w_+) along the eigenvector corresponding to the real negative eigenvalue, and this enables a detailed numerical investigation via shooting (e.g. Atkinson et al. 2009, §11.2.2).

My numerical method was to solve (2a) backwards in x , starting close to (u_+, w_+) on the eigenvector corresponding to the real negative eigenvalue. General theory shows that for greatest accuracy, the distance between the starting point and the steady state should scale with the square root of the local numerical error (Sherratt et al. 2010, Appendix B). Figure 5a–c shows the form of this solution as A is varied, when $B = 0.45$ and $v = 5$. When A is small, the solution terminates at the unstable steady state (u_-, w_-) , and when A is larger it terminates at infinity. The critical value $A_{crit,1}$ delimits these two behaviours. This is shown in Fig. 5b; of course the starting point for this solution is not exactly on the stable manifold of (u_+, w_+) , and consequently the numerical solution in Fig. 5b ultimately moves away from $(0, A)$ after coming very

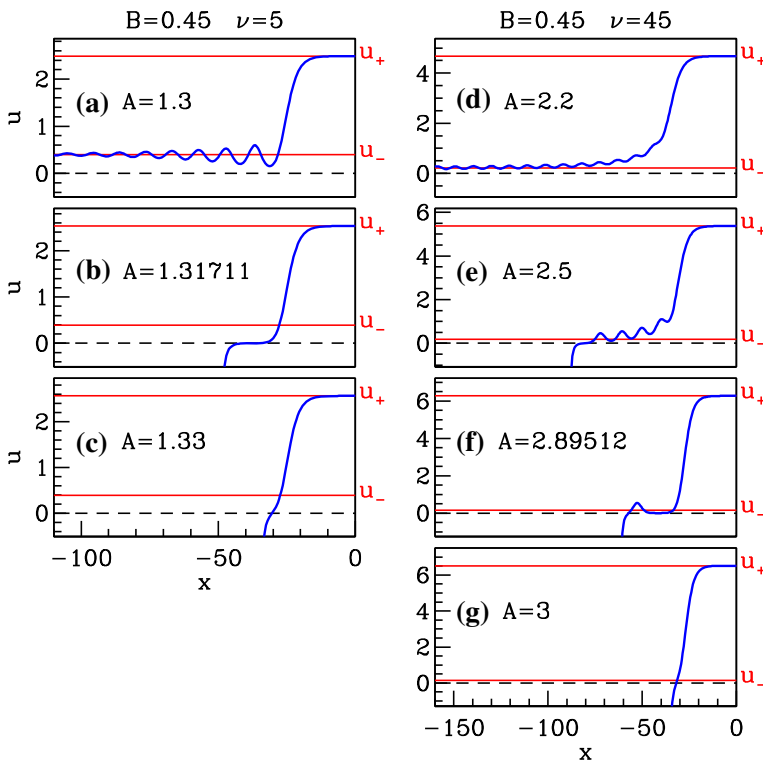


Fig. 5 Examples of the use of numerical shooting to calculate the critical value $A_{crit,1}$ of the rainfall parameter A above which vegetation can spread in the downhill direction. The plots are numerical solutions for u of (2a), solved backwards in x starting close to (u_+, w_+) on the eigenvector corresponding to the (unique) real negative eigenvalue. I omit the corresponding solutions for w , for brevity. For smaller values of v such as in the left hand column, $A_{crit,1}$ corresponds to a transition between this solution terminating at (u_-, w_-) and at infinity. For larger values of v such as in the right hand column, $A_{crit,1}$ corresponds to a transition between the solution terminating at $(0, A)$ but with a non-monotonic form, and terminating at infinity

close to it. Nevertheless, the transition between the solution approaching (u_-, w_-) and infinity enables easy numerical estimation of $A_{crit,1}$.

This behaviour is typical when ν is small but for larger values of ν the sequence is more complicated, as illustrated in Fig. 5d–g for $B = 0.45$ and $\nu = 45$. Again there are two cases: the solution terminates at (u_-, w_-) for small A and at infinity for large A . However my solutions suggest that there is now a range of intermediate values of A for which the solution terminates at $(0, A)$ (Fig. 5e, f). The plot in Fig. 5e is typical for such values of A : the solution is non-monotonic in u (and w , not shown). Rough estimates of $A_{crit,1}$ made via the direction of interface movement in numerical solutions of (1) suggest that $A_{crit,1}$ corresponds to the transition between these non-monotonic solutions and solutions that terminate at infinity (Fig. 5g), and that at this critical value the solution is monotonic. Again this enables easy numerical estimation of $A_{crit,1}$. To avoid confusion I repeat the remark made earlier in connection with Fig. 5b, that the numerical solutions shown in Fig. 5e, f ultimately tend to infinity after passing very close to $(0, A)$ because the starting point is not exactly on the stable manifold of (u_+, w_+) . Concerning the family of non-monotonic solutions connecting (u_+, w_+) and $(0, A)$, I hypothesise that these are all unstable as solutions of (1). This hypothesis is quite plausible given the various results of the form ‘nonmonotonicity implies instability’ that are known for scalar reaction-diffusion equations (Hagan 1981; Henry 1981), but I leave a detailed investigation of this for possible future work.

My characterisation of $A_{crit,1}$ as a transition value for the solutions of (2a) again makes it straightforward to obtain accurate numerical estimates of this critical value. Figure 6 shows a typical example of the variation of $A_{crit,1}$ with ν .

I now consider interfaces with the bare ground state $(0, A)$ on the uphill side ($x \rightarrow +\infty$) and the uniformly vegetated state (u_+, w_+) on the downhill side ($x \rightarrow -\infty$), as illustrated schematically in Fig. 3b. Note that this scenario implicitly imposes the restriction $A \geq 2B$, which is required for the existence of the vegetated state (u_+, w_+) . For large ν , numerical simulations of (1) show that this type of interface evolves to a travelling wave front that always moves in the uphill direction; intuitively, the downhill flow of water is sufficient to enable vegetation spread even at the minimum rainfall level $A = 2B$. However for smaller ν the travelling wave velocity passes through zero at a second critical value $A_{crit,2}$. Again this is consistent with intuitive and mathematical expectations. The downhill flow of water will facilitate the spread of vegetation in this case, whereas it impedes vegetation spread for the interfaces considered in the previous paragraphs, which have vegetation on the uphill side and bare ground on the downhill side. Therefore one expects that $A_{crit,2} < A_{crit,1}$, and this is confirmed in simulations.

Again, at $A = A_{crit,2}$ there will be a stationary transition front, satisfying (2a), and my previous investigation of eigenvalues shows that this front must approach $(0, A_{crit,2})$ along the eigenvector corresponding to the negative eigenvalue $-B^{1/2}$. Again this enables numerical calculation of the front solution via shooting, and in this case the situation is straightforward. For large A the solution starting on this eigenvector terminates at (u_-, w_-) , while for small A it terminates at infinity (not illustrated for brevity). The critical value $A_{crit,2}$ is the threshold between these two behaviours, and this enables straightforward numerical estimation. An example of

the variation of $A_{crit,2}$ with ν is shown in Fig. 6; this figure uses $B = 0.45$ but my calculations suggest that the qualitative form is independent of $B (< 2)$. Note that the $A_{crit,2}$ locus in this figure terminates at $\nu \approx 1.55$, when $A_{crit,2} = 2B$. For larger values of ν transition fronts of the type illustrated in Fig. 3b always move in the uphill direction. Note also that when $\nu = 0$ the two types of interface are identical and therefore $A_{crit,1} = A_{crit,2}$. Their common value can in fact be calculated exactly: it is a special case of a problem on waves of desertification studied by [Sherratt and Synodinos \(2012\)](#). Briefly, when $\nu = 0$ (2b) can be rewritten to give w as a function of u , so that (2a) reduces to a single ODE for u which can be solved exactly.

The plots of $A_{crit,1}$ and $A_{crit,2}$ in Fig. 6 divide the ν – A parameter plane into four regions. In region I vegetation cannot spread in either the uphill or downhill direction, so that a localised patch of vegetation collapses (as in Fig. 2f). In region II vegetation will spread uphill but not downhill: thus both edges of a localised vegetation patch

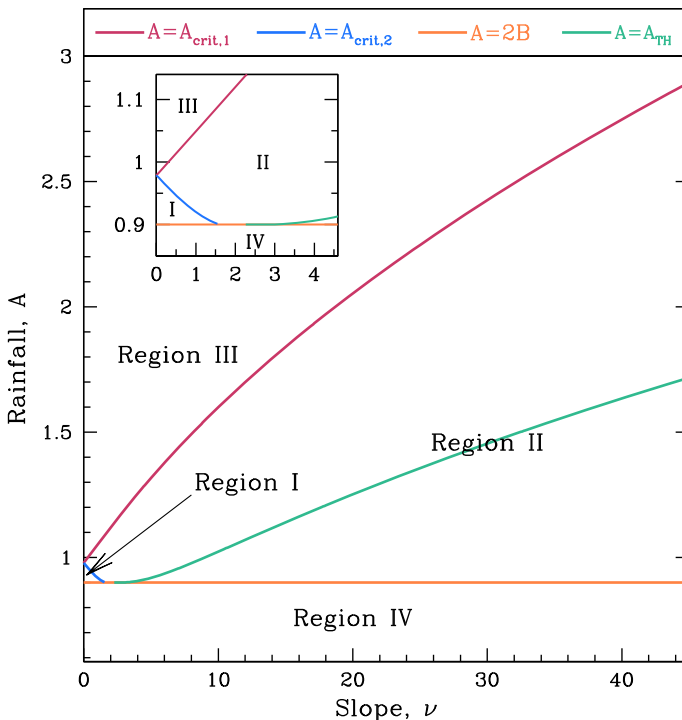


Fig. 6 A division of the ν – A parameter plane into regions with qualitatively different behaviours following a localised introduction of vegetation on a bare hillslope, for $B = 0.45$. In region I a localised patch of vegetation collapses because vegetation cannot spread in either the uphill or downhill direction (e.g. Fig. 2f). In region II both edges of the patch migrate uphill so that colonisation does not occur (e.g. Fig. 2b–d). In region III the patch will spread in all directions, so that colonisation occurs (e.g. Fig. 2a). Finally in region IV $A < 2B$ so that there is no uniformly vegetated state: here vegetation dies out, either via collapse or via uphill migration (e.g. Fig. 2e). Region II is subdivided by the locus of Turing–Hopf bifurcation points. *Below this line* patterns form within the vegetation as it migrates uphill (e.g. Fig. 2c, d); *above the line* vegetation remains uniform (e.g. Fig. 2b)

spread uphill (as in Fig. 2b–d). In region III vegetation will spread in both the uphill and downhill directions, so that colonisation occurs (as in Fig. 2a). Finally in region IV $A < 2B$ so that there is no uniform vegetated state: here vegetation dies out, either via collapse or via uphill migration (as in Fig. 2e). Figure 6 also shows the locus of Turing–Hopf bifurcation points A_{TH} . This is easily calculated via linear stability analysis (Sherratt 2005; van der Stelt et al. 2013) and is the maximum value of rainfall A at which patterns exist (Sherratt 2013a; Siteur et al. 2014b). The key result is that this thick line lies entirely below region III in which colonisation occurs. This implies that colonisation cannot generate spatial patterns. I repeated the calculations in Fig. 6 for $B = 0.1, 0.2, \dots, 2.0$ (recall that B is constrained to lie between 0 and 2); the qualitative form of the plot is the same in all cases, so that my conclusion is quite general.

4 Colonisation with water diffusion

I have shown that in the absence of water diffusion ($D = 0$), colonisation of a uniform slope cannot generate patterned vegetation. However when water diffusion is included in the model (1), this is no longer true. Figure 7 shows the results of model simulations when a localised region of vegetation is introduced onto a bare uniform slope when $D = 100$, for different values of the rainfall parameter A . The initial vegetation simply collapses when A is sufficiently small (Fig. 7a). At slightly larger A both upslope and downslope edges of the vegetation patch move in the uphill direction (Fig. 7b), and then at sufficiently large A the downslope edge begins to move downhill, heralding colonisation (Fig. 7c). However in contrast to the behaviour when $D = 0$, the colonising vegetation is patterned, with a transition to colonisation by uniform vegetation at larger rainfall levels (Fig. 7d). Intuitively, water diffusion increases flow from unvegetated to vegetated regions, and thus enhances the pattern-forming potential of the system. Consequently water diffusion increases the maximum rainfall level for pattern formation, and at a sufficiently high diffusion coefficient this maximum rainfall level exceeds that required for colonisation.

As in Sect. 3 this behaviour can be investigated in detail by considering interfaces between the desert state $(0, A)$ and the uniformly vegetated state (u_+, w_+) in one space dimension (no y dependence). Again, colonisation occurs at values of rainfall A above the critical value A_{crit} at which there is a stationary front with $(0, A)$ on the downhill side and (u_+, w_+) on the uphill side. However the ODEs satisfied by this stationary front are now fourth order, and numerical calculation of eigenvalues indicates that the stable and unstable manifolds are both two-dimensional at both $(0, A)$ and (u_+, w_+) . This means that the straightforward numerical shooting approach that I used to calculate $A_{crit,1}$ and $A_{crit,2}$ (when $D = 0$) cannot be used for A_{crit} . Instead I based my calculation on simulations of the PDEs (1). This is much more expensive in computer time, so that one cannot cover such a large number of parameter sets as in Sect. 3.

I solved (1) with step function initial conditions $u(x, t = 0) = (u_+, w_+)$ for $x > 0$ and $(0, A)$ for $x < 0$. The solution evolves to a transition front moving with constant shape and velocity. I calculated this velocity numerically, and then regarded

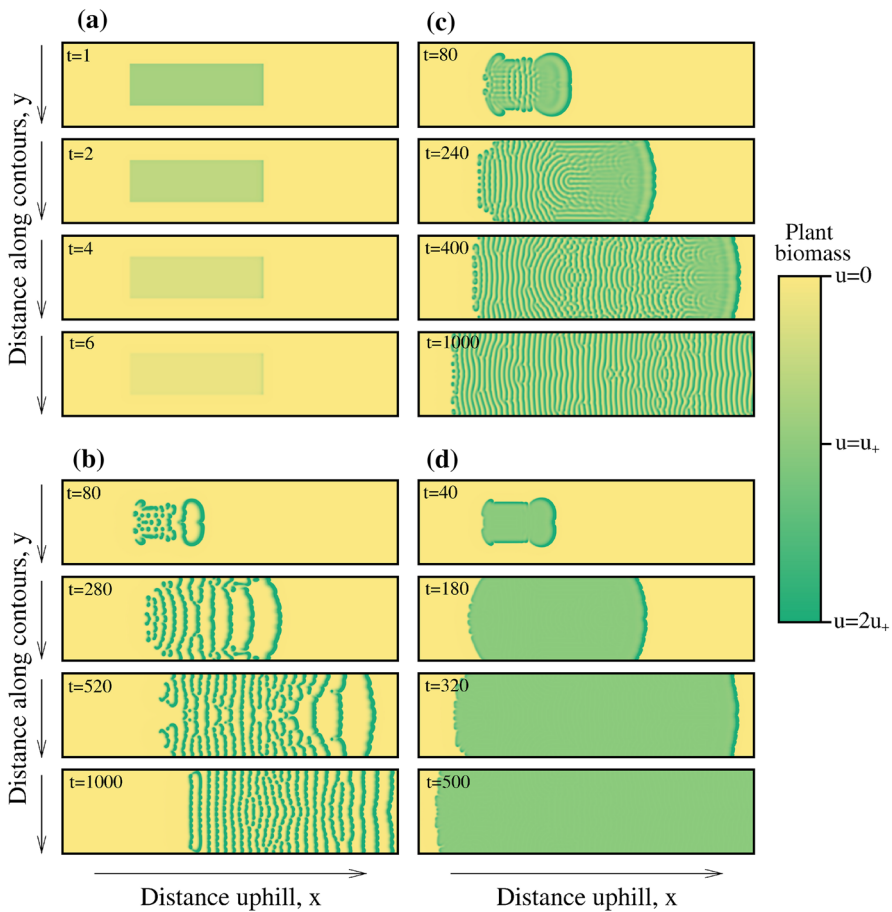


Fig. 7 The dynamics of a localised patch of vegetation on a uniform hillslope, as predicted by the model (1) with the water diffusion term included. Colonisation occurs in **c** and **d** since the vegetation patch expands in both the uphill and downhill directions. In **b** there is no colonisation because both the upslope and downslope edges of the patch move uphill, while in **a** the vegetation simply collapses. The plotted region is $0 < x < 750, 0 < y < 182.5$. In **b–d** I set $u(x, y, t = 0) = u_+$ when $150 < x < 250$ and $73 < y < 109.5$ with $u(x, y, t = 0) = 0$ otherwise; $w(x, y, t = 0) \equiv A$. In **a** the initial vegetation patch is larger to give greater visual clarity: $150 < x < 450$ and $45.5 < y < 137$. The parameters are $B = 0.45, v = 16$ and $D = 100$, with A as indicated. The shading denotes vegetation density, as shown in the scalar bar. In **a** I solve the equations on the plotted region, but in **b–d** the solution domain extends to $x = 2000$ (though only $0 < x < 750$ is plotted) in order that vegetation does not invade to the right hand boundary. The boundary conditions are periodic in y and Dirichlet ($u = 0, w = A$) at $x = 0$ and $x = 750$, **b–d** $x = 2000$. The equations were solved using an alternating direction implicit finite difference method with upwinding, with a uniform grid spacing of 0.5 and a time step of 1.25×10^{-3}

it as a function of A , using a numerical bisection method to solve for the value of A at which the velocity is zero: this is A_{crit} . The relatively long run times for each simulation² mean that in practice the accuracy of this procedure is limited by the

² The numerical details of my implementation are as follows. I solve (1) using a semi-implicit finite difference scheme with upwinding, using a grid spacing $\delta x = 0.5$ and a time step $\delta t =$

number of iterations that can be performed in the numerical bisection procedure. My implementation is accurate to about $\pm 10^{-3}$.

Figure 8 plots A_{crit} against ν for four values of the water diffusion coefficient D . Note that for any given values of A and D , there is a critical value of ν above which colonisation does not occur. This is consistent with field data from a wide range of environments showing that there are threshold levels of slope angle above which plant colonisation does not occur; this includes in particular studies of semi-arid parts of Spain (Cantón et al. 2004; Bochet et al. 2009). Superimposed on the plots in Fig. 8 are the loci of pattern onset (Turing–Hopf bifurcation) points: patterns occur for values of A below this locus. For D sufficiently small (below about 10) A_{crit} is above the pattern onset locus for all ν , so that colonisation cannot generate spatial patterns—as for the case of $D = 0$ discussed in Sect. 3. But for larger values of D , A_{crit} lies below the pattern onset locus when ν is sufficiently small, implying that colonisation generates spatial patterns. The upper limit on ν for this to occur increases with D , and this is shown more clearly in Fig. 9 which plots results for five values of the plant loss parameter B .

5 Colonisation in the Rietkerk model

The previous sections of the paper have all concerned Klausmeier's (1999) model (1) for semi-arid vegetation. It is natural to ask whether my conclusions are restricted to this model, or whether they apply more generally. To address this question, I now consider colonisation in the Rietkerk model (HilleRisLambers et al. 2001; Rietkerk et al. 2002). This is widely used in modelling studies of vegetation patterning (e.g. Kéfi et al. 2008; Dagbovie and Sherratt 2014; Yizhaq et al. 2014; Bonachela et al. 2015), and like the Klausmeier model it is based on the water redistribution hypothesis for semi-arid vegetation patterning (see Sect. 1). The key difference between the two models is that Rietkerk's formulation uses separate water variables: soil water W and surface water O . This is more realistic since the kinetic and transport properties are both different for soil and surface water. Nevertheless it remains a major simplification since in reality the dynamics of soil water are three-dimensional and are modulated by spatiotemporal variability in rooting depth (Nippert and Knapp 2007a, b; Schwinning 2010). The equations governing these water variables and the plant biomass P are:

Footnote 2 continued

$\min\{0.8\delta x/\nu, 0.1\delta x^2/\max\{D, 1\}\}$; here the factor of 0.8 ensures that the CFL number is less than 1. I solve on a space domain of length 500 with Dirichlet conditions $(u, w) = (0, A)$ at $x = -250$ and $(u, w) = (u_+, w_+)$ at $x = 250$. I solve over a time interval of length 1000. For the first iteration of the bisection method I use initial conditions $(u, w) = (0, A)$ on $-250 < x < 0$ and $(u, w) = (u_+, w_+)$ on $0 < x < 250$. For subsequent iterations I use the final solution form from the previous iteration, translated to be centred at $x = 0$: this accelerates convergence to the travelling wave profile. I estimate the velocity of this wave via the distance travelled over the final 100 time units, or over an earlier 100 time units if the front reaches an end of the domain before the end of the solution period. I terminate my numerical bisection method when two successive values of A differ by less than 10^{-3} .

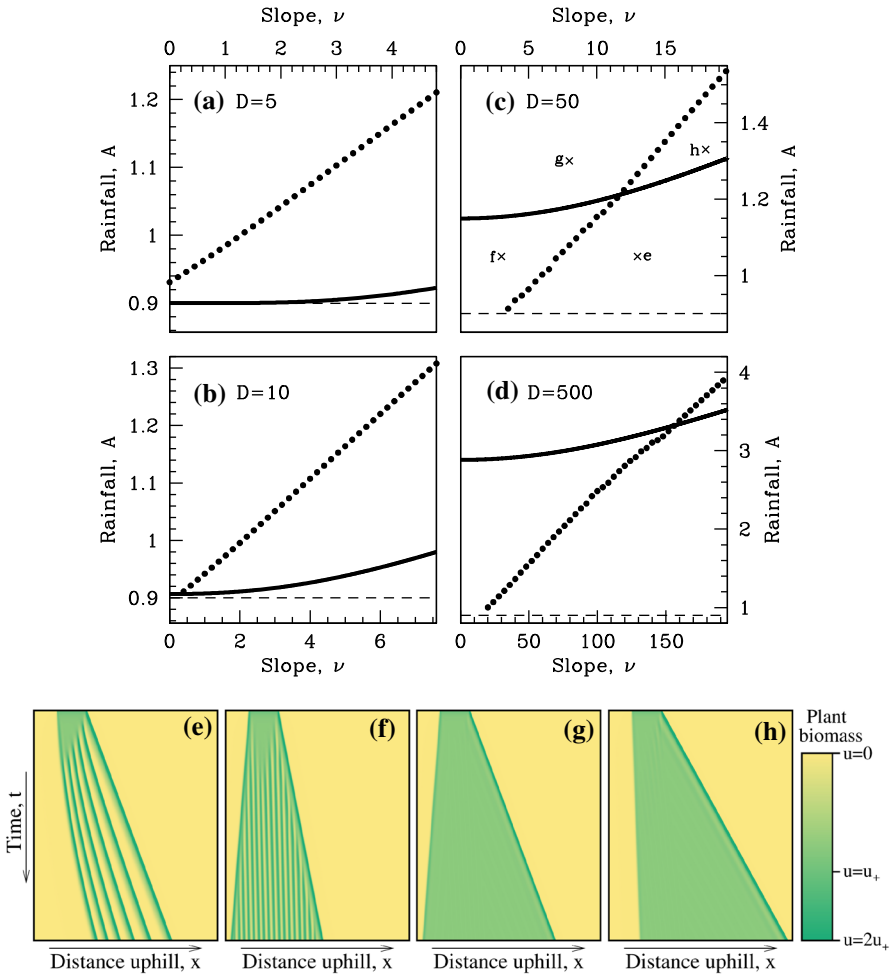


Fig. 8 Parameter conditions for vegetation patterning following colonisation. **a–d** The *solid line* shows the critical value of A below which patterns occur, and the *dots* show A_{crit} , the value of A above which colonisation occurs. Therefore colonisation generates vegetation patterns when the *dots* lie below the *solid line*. The *dashed line* is $A = 2B$, which is the minimum rainfall level for existence of the vegetated steady state (u_+, w_+) . The plant loss parameter $B = 0.45$. As an aid to interpretation, I show space–time plots of simulations of (1) in one space dimension (no y dependence) for $D = 50$. The values of A and ν are as indicated in **c**: **e** $A = 1.05$, $\nu = 13$; **f** $A = 1.05$, $\nu = 3$; **g** $A = 1.3$, $\nu = 8$; **h** $A = 1.33$, $\nu = 18$. The *shading* indicates plant biomass, as shown in the *scalebar*. I solve for $0 < t < 250$ and $0 < x < 600$ with Dirichlet boundary conditions ($u = 0$, $w = A$). At $t = 0$ I set $u = u_+$ on $75 < x < 175$, with $u = 0$ otherwise; $w(x, t = 0) = A$ for all x . The equations were solved using a finite difference method with upwinding, with a uniform grid spacing of 0.5 and a time step of 0.0005

$$\begin{aligned}
 \text{Plant biomass} \quad \frac{\partial P}{\partial T} = & \underbrace{D_P \frac{\partial^2 P}{\partial X^2}}_{\text{plant dispersal}} + \underbrace{C g_{max} \frac{W}{W + k_1} P}_{\text{plant growth}} - \underbrace{dP}_{\text{plant loss}} \quad (4a)
 \end{aligned}$$

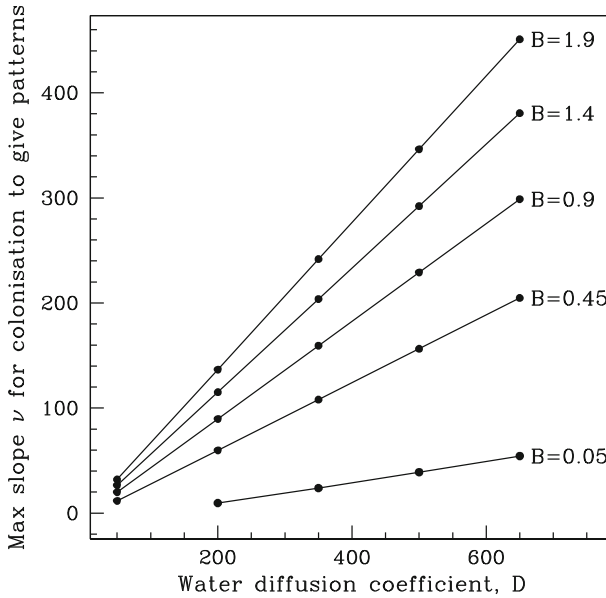


Fig. 9 The critical value of slope ν below which colonisation generates patterned vegetation, as a function of water diffusivity D . Figure 8 demonstrates that when D is greater than about 10, colonisation leads to patterned vegetation on sufficiently shallow slopes. This figure plots the upper limit on ν for $B = 0.45$ as used in Fig. 8 and also for four other values of B . I calculated the critical value of ν from results such as those illustrated in Fig. 8, using linear interpolation to estimate when $A = A_{crit}$ crosses the pattern onset (Turing–Hopf) locus. When $B = 0.05$ and $D = 50$ colonisation generates uniform vegetation for all slopes $\nu \geq 0$, and hence no data point is plotted

$$\begin{aligned}
 \text{Soil water } \partial W/\partial T = & \underbrace{D_W \partial^2 W/\partial X^2}_{\text{soil water flow}} + \underbrace{\alpha O \frac{P + k_2 W_0}{P + k_2}}_{\text{infiltration of surface water}} - \underbrace{g_{max} \frac{W}{W + k_1}}_{\text{water uptake by plants}} P - \underbrace{r_W W}_{\text{evaporation and drainage}} \quad (4b)
 \end{aligned}$$

$$\begin{aligned}
 \text{Surface water } \partial O/\partial T = & \underbrace{D_O \partial^2 O/\partial X^2}_{\text{surface water diffusion}} + \underbrace{\mu \partial O/\partial X}_{\text{flow downhill}} - \underbrace{\alpha O \frac{P + k_2 W_0}{P + k_2}}_{\text{infiltration of surface water}} + \underbrace{R}_{\text{rainfall}} \quad (4c)
 \end{aligned}$$

Here T is time and X is space, running in the uphill direction. In view of the longer run times for simulations of (4a) compared to (1), I restrict attention to a one-dimensional domain; this restriction is reasonable in light of my work on the Klausmeier model earlier in the paper, where the key phenomena can be seen and understood in one space dimension.

The various model parameters and their interpretations are listed in Table 1. Note in particular that the known positive correlation between vegetation cover and the infiltration of rainwater (Rietkerk et al. 2000; Thompson et al. 2010) is reflected in the

Table 1 Ecological interpretations of the parameters in the Rietkerk model (4a)

Parameter	Value	Interpretation
C	10	Conversion of water uptake into new biomass
g_{max}	0.05	Maximum water uptake per unit of biomass
k_1	5	Half-saturation constant for water uptake
D_P	0.1	Plant dispersal coefficient
α	0.2	Maximum infiltration rate
k_2	5	Saturation constant for water infiltration
W_0	0.2	Water infiltration rate without plants
r_W	0.2	Specific rate of evaporation and drainage
D_W	0.1	Diffusion coefficient of soil water
d	0.25	Per capita death rate of plants
μ	Varied	Advection coefficient for downslope water flow
R	Varied	Mean rainfall
D_O	Varied	Diffusion coefficient of surface water

In this paper I vary R , μ and D_O and keep the other parameters fixed at the values given in the table, which are also the values given by Rietkerk et al. (2002). It should be noted that the parameters are dimensional, and a useful tabulation of the units for all variables and parameters is given in HilleRisLambers et al. (2001). Since I am not making any use of the dimensional values in this paper, I omit the units when giving numerical values

term $(P + k_2 W_0)/(P + k_2)$ ($W_0 < 1$). Note also that as in the Klausmeier model (1), plant growth rate is assumed to be proportional to the uptake of soil water by plants; this is taken to have a Michaelis–Menten dependence on soil water. The number of parameters in (4a) clearly precludes any attempt at a systematic study. Therefore I will fix all parameters at the values given in Rietkerk et al. (2002) and listed in Table 1, with the exception of the rainfall R , the slope μ and the water diffusion coefficient D_O , which I vary. Note that I focussed on variations in corresponding parameters in the Klausmeier model (1) in Sects. 3 and 4.

My main conclusion in Sect. 3 was that for the Klausmeier model (1) without water diffusion, colonisation always generates uniform rather than patterned vegetation. However for the Rietkerk model (4a) this is not the case. Figure 10a–d shows simulations of (4a) with $D_O = 0$ for different rainfall levels R , when a localised region of vegetation is imposed on otherwise bare ground. At very low rainfall, the initial vegetation patch collapses (not shown in Fig. 10). At larger rainfall levels the patch aggregates and migrates uphill (Fig. 10a), and then above a critical rainfall level the patch forms into distinct bands, and also a succession of new bands are initiated on the downhill side of the patch's initial location (Fig. 10b). This is an example of colonisation, with the resulting vegetation being patterned. Further increases in rainfall cause the patch to spread as uniform vegetation rather than bands, although new bands are still initiated on the downhill side of the patch's initial location (Fig. 10c). Finally at sufficiently high rainfall levels, uniform vegetation spreads in both the uphill and downhill directions (Fig. 10d). The small oscillations in the downhill spread of vegetation in Fig. 10d are a vestige of the initiation of new bands that occurs in Fig. 10b,

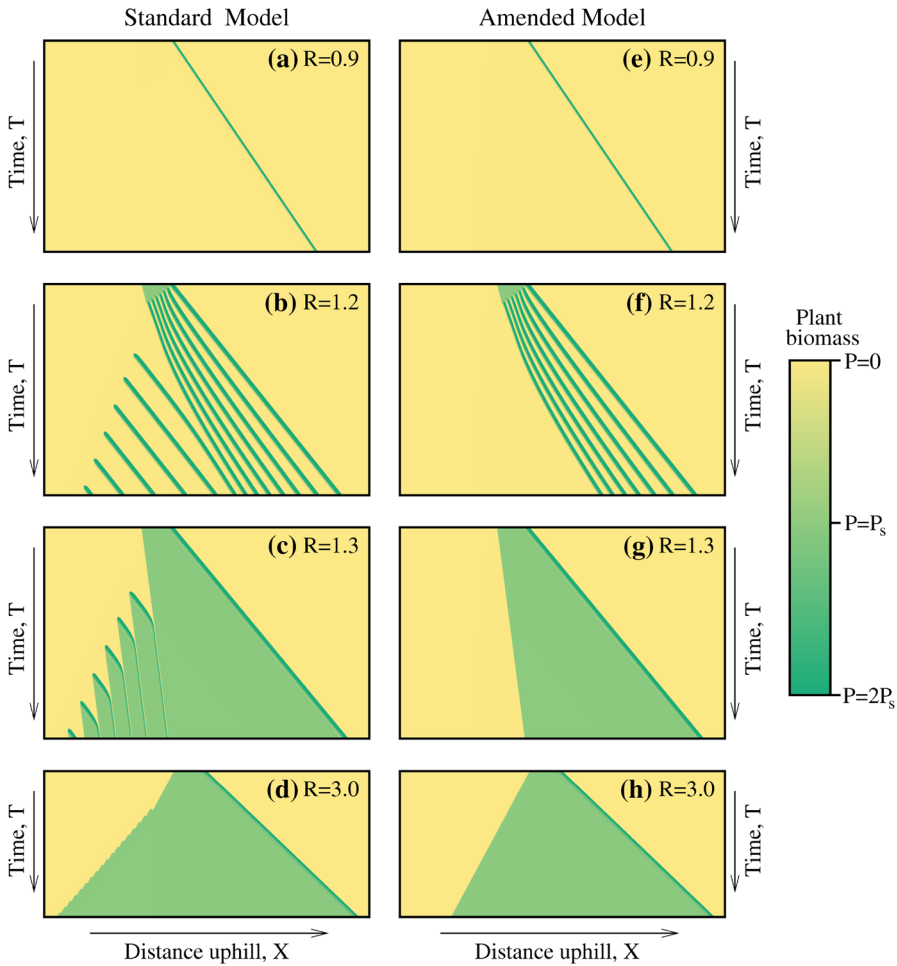


Fig. 10 Colonisation in the Rietkerk model (4a) when the surface water diffusion coefficient $D_O = 0$. **a–d** The dynamics of a localised patch of vegetation on a uniform hillslope, as predicted by the standard model. **e–h** The corresponding solutions of the amended model, in which the kinetic terms in the P equation are set to zero when $P < 10^{-3}$. The slope parameter $\nu = 4$, with the values of rainfall R as indicated on the solution panels, and with other parameters as given in Table 1. The shading indicates plant biomass, as shown in the scalebar. The spatial domain is $0 < X < 5000$ and the solution is shown up to **a–c, e–g** $T = 13,000$, **d, h** $T = 9000$; the geometry of the plots in **d, h** reflects the different time interval. The initial vegetation patch is of length 500, with downhill edge at **a–c, e–g** $X = 1500$, **d, h** $X = 2000$; given the faster downhill migration for $R = 3$, this difference extends the time before the whole domain is colonised. Since I stop the simulations before this occurs, I use Dirichlet boundary conditions with variables set to the desert steady state. The equations were solved using a finite difference method with upwinding, with a uniform grid spacing of 0.5 and a time step of 0.1; these give a CFL number of 0.8

c. The key result here is Fig. 10b, which shows colonisation-induced patterning even though $D_O = 0$; this appears to contradict the predictions of the Klausmeier model discussed in Sect. 3. Admittedly there is a non-zero diffusion term in the soil water equation, and it is important to clarify that there is no precise relationship between the

parameter D in the Klausmeier model and the parameters D_O and D_W in the Rietkerk model. Nevertheless the model (4a) with $D_O = 0$ can be considered broadly equivalent to (1) with $D = 0$ since in both cases setting the diffusion coefficient to zero prevents pattern formation on flat terrain ($\mu = 0$ and $\nu = 0$ respectively). Moreover, setting $D_W = 0$ (as well as $D_O = 0$) actually has a negligible effect on results such as those shown in Fig. 10a–d.

In fact the occurrence of colonisation-induced patterning in (4a) can be explained very simply by considering the stability of spatially uniform steady states, which are a “vegetated” state (P_s, W_s, O_s) and a “desert” state $(P, W, O) = (0, R/r_w, R/(\alpha W_0))$. Here

$$W_s = \frac{dk_1}{Cg_{max} - d} \quad P_s = \frac{R - r_w W_s}{g_{max} W_s} (W_s + k_1) \quad O_s = \frac{R}{\alpha} \frac{P_s + k_2}{P_s + k_2 W_0}.$$

These two steady states meet at a transcritical bifurcation, which occurs at $R = 1$ for the parameter values listed in Table 1. For $R < 1$ the desert state is stable to homogeneous perturbations while the vegetated state is unstable. For $R > 1$ the opposite applies: the desert steady state is unstable and the vegetated state is stable (to homogeneous perturbations). Note also that $P_s < 0$ for $R < 1$ so that the vegetated steady state is not ecologically relevant. This stability profile is quite different from that in the Klausmeier model, in which the desert state is stable for all parameters. This difference has major implications for colonisation. In the Klausmeier model transition fronts between the desert state and either uniform or patterned vegetated states are between two stable states, so that the direction of movement can be expected to be parameter-dependent. However in the Rietkerk model with $R > 1$ and other parameters as in Table 1, the desert state is unstable, so that one necessarily expects it to be invaded by either uniform or patterned vegetation in both the uphill and downhill directions. This is analogous to the difference between travelling wave fronts in the Fitzhugh–Nagumo equation and the Fisher equation (Murray 2003). Thus one expects colonisation to occur whenever $R > 1$, exactly as is seen in Fig. 10a–d. In Fig. 10b, c the spread of the vegetation occurs via a simple transition front in the uphill direction, but via an oscillatory front in the downhill direction.

This understanding of the results in Fig. 10a–d raises a natural approach to reconciling the two models. The oscillatory spread of vegetation in the downhill direction in Fig. 10b, c involves the slow growth of vegetation from a density close to zero, until a vegetation band is initiated and the density drops again to close to zero. This intuitive description, which is based only on observations of the simulation results, suggests that the oscillatory downhill spread depends on the growth of plant density when this is very small—possibly too small to be of real ecological significance. Therefore I amended the model (4a) by setting the kinetic terms in the P equation to zero whenever $P < \epsilon$ for some small threshold ϵ . This type of cut-off has been used for other PDE models of population dynamics by a number of previous authors to avoid phenomena that arise from meaninglessly low population densities (Gurney et al. 1998; Cruickshank et al. 1999; Popović 2011; Benguria and Depassier 2014). I arbitrarily fix the default value of ϵ at 10^{-3} , but increasing or decreasing ϵ by as much as two orders of magnitude has no visible effect on the solutions. Figure 10e–h shows the solutions corresponding

to those in Fig. 10a–d, but with this amended model. The initiation of new vegetation bands on the downhill side of the initial patch, which occurs in Fig. 10b–d, is absent in the corresponding simulations of the amended model (Fig. 10f–h), but otherwise the results are unaffected by the imposition of the threshold.

The results in Fig. 10e–h are consistent with those for the Klausmeier model with $D = 0$, and this holds for all of the simulations that I have done for other values of μ and R . That is, the amended Rietkerk model also predicts that in the absence of water diffusion ($D_O = 0$), colonisation of bare ground always generates uniform vegetation rather than patterns. When considering this prediction, one must ask: how realistic is my amendment to the Rietkerk model? Effectively, my amendment is equivalent to an extremely slight weak Allee effect (Courchamp et al. 2008). There is a large body of literature on Allee effects in populations of both wind- and insect-pollinated plants (e.g. Davis et al. 2004; Duffy et al. 2013). These studies demonstrate significant reductions in per capita growth rate at low population densities for some plant species, but this is certainly species-dependent. However a cessation of plant growth at extremely low densities is a reasonable general assumption. It should be noted that my amendment to the model does not affect any of the simulations in Rietkerk et al.'s (2002) original paper, since these concern patterns forming via the disruption of uniform vegetation, so that the vegetation density never approaches zero.

I now consider colonisation in the Rietkerk model (4a) when $D_O > 0$, retaining my amendment of zero P kinetics when $P < \epsilon = 10^{-3}$. Again my aim is to investigate whether model simulations agree with the predictions of the Klausmeier model (1). I ran a large number of simulations in which I imposed a localised patch of vegetation on an otherwise bare uniform slope, varying the slope μ , the rainfall R , and the surface water diffusion coefficient D_O , with the other parameters fixed at the values given in Table 1. In each case I noted whether or not colonisation occurred, and whether the vegetation was uniform or patterned; there is an additional possible outcome of collapse, which occurs at very low rainfall levels. I found that provided D_O is sufficiently large (greater than about 0.5), colonisation generates patterned vegetation for some levels of rainfall on sufficiently shallow slopes (Fig. 11). The threshold slope for colonisation-induced patterning increases with the surface water diffusion coefficient D_O (compare parts a and b of Fig. 11). These predictions are in complete accord with those of the Klausmeier model (see Sect. 4). Since the two models are quite different mathematically, this suggests that the predictions are a consequence of the basic underlying assumption of water redistribution as the pattern generation mechanism.

6 Discussion

In the extensive literature on mathematical modelling of vegetation patterns, there is almost no discussion of pattern generation via the colonisation of bare ground. Instead, attention has focussed on patterns that arise from the degradation of spatially uniform vegetation. The present paper is a preliminary attempt to rectify this omission. I have shown that colonisation always generates uniform rather than patterned vegetation in the absence of water diffusion. However when a sufficiently large water diffusion term is included, colonisation does generate patterns on shallow slopes. These conclusions

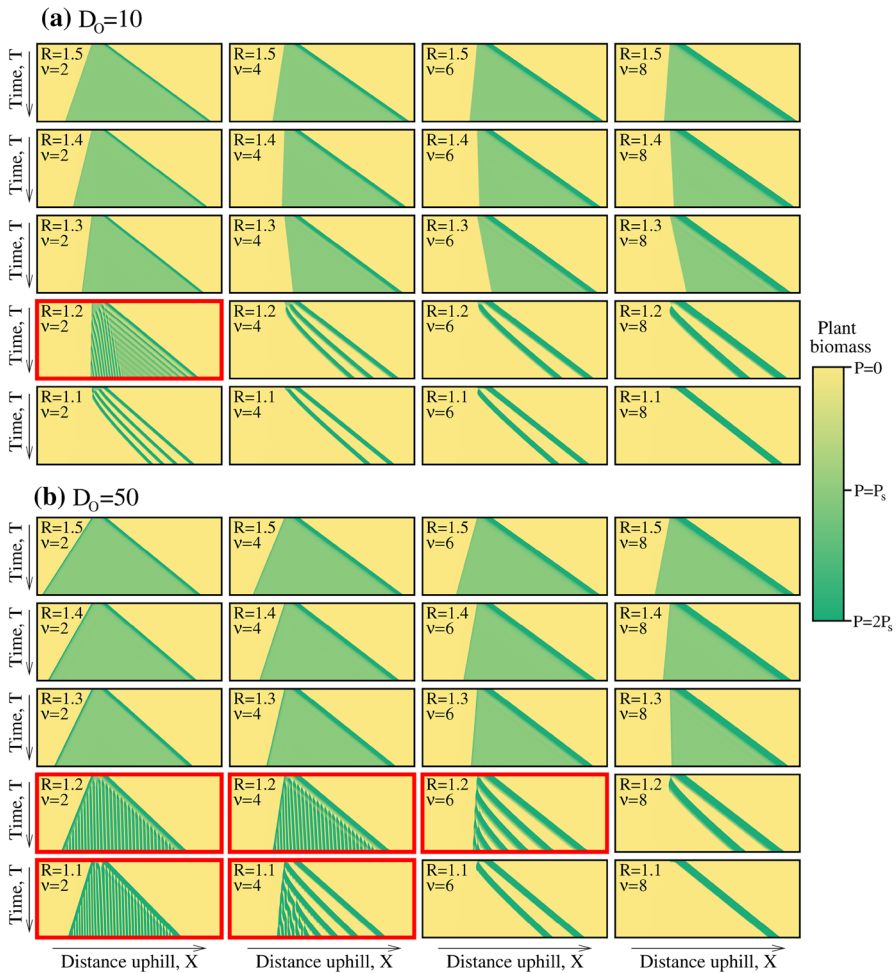


Fig. 11 Colonisation in the Rietkerk model (4a) with surface water diffusion. I show the dynamics when a localised patch of vegetation is imposed on an otherwise bare uniform hillslope for a grid of values of the slope ν and the rainfall R , for **a** $D_0 = 10$, **b** $D_0 = 50$. The other parameters are as in Table 1. The shading indicates plant biomass, as shown in the scalebar. I use the amended version of (4a) in which the kinetic terms in the P equation are set to zero when $P < 10^{-3}$. The panels with highlighted borders are those for which colonisation occurs and generates patterns. The spatial domain is $0 < X < 2260$ and the solutions are shown up to $T = 6333$. The initial vegetation patch is $670 < X < 850$. The equations were solved using a finite difference method with upwinding, with a uniform grid spacing of 0.5 and a time step of **a** 0.0025, **b** 0.0005. Comparison of this figure with Fig. 8 shows the close qualitative correspondence between the predictions of the Klausmeier and Rietkerk models

apply both for the Klausmeier model and for the amended Rietkerk model. An important question is how these conditions on water diffusion coefficient and slope compare with values that are appropriate for real semi-arid ecosystems.

The ability of the extended Klausmeier model (1) to generate spatial patterns on flat ground, in contrast to Klausmeier's (1999) original formulation, was first highlighted

by Kealy and Wollkind (2012). However those authors did not attempt to estimate the water diffusion coefficient D in (1), and to my knowledge only two previous papers have done this. Ursino (2005) used the Richards equation for soil water flow to obtain an expression for D in terms of soil parameters, leading to estimates of D between 7.5 and 110. Siteur et al. (2014b) obtained the larger estimate of 500 by comparing the rainfall range giving patterns in the model and in field data. Consequently there remains considerable uncertainty about the appropriate value of D , but almost all of these previous estimates are large enough to enable colonisation-induced patterning on sufficiently shallow slopes. The value of the slope parameter clearly depends on the gradient of the slope being considered. Banded vegetation is restricted to shallow slopes, c. 0.2–2 % (Valentin et al. 1999; Deblauwe et al. 2012); on steeper slopes rainfall generates gullies rather than moving via sheet flow. As for D , estimates for the slope parameter ν are limited and variable. Most previous studies (including much of my own work) follow Klausmeier's (1999) original paper and use $\nu = 182.5$, even though the paper contains no justification for this value. Ursino's (2005) calculations based on the Richards equation give estimates between 3 and 40 times the percentage slope.

In view of this variability and uncertainty one cannot make definitive statements, but it is clear that the generation of vegetation patterns by colonisation is at least a realistic possibility in real ecosystems. Moreover it is notable that the D – ν pair used in the recent study of Siteur et al. (2014b) and the typical pairs implied by Ursino's (2005) calculations are both consistent with colonisation-generated patterns.

For the Rietkerk model, almost all previous applications concern flat ground. Two exceptions are the original paper of Rietkerk et al. (2002), who take $\mu = 10$ (units: m day^{-1}), and Thompson and Katul (2009), who take $\mu = 2$ (units: m day^{-1}). In neither case is the value justified in any way, and both papers set $D_O = 0$. The only previous paper that I am aware of that uses (4a) with μ and D_O both non-zero is Dagbovie and Sherratt (2014), in which Rietkerk's value $\mu = 10$ is used, and D_O is varied between 0 and 100. The maximum value of 100 (units: $\text{m}^2 \text{day}^{-1}$) in that paper is chosen simply because it is the value used by Rietkerk et al. (2002) on flat ground, which itself has no clear justification. In summary there is really no good ecological basis for the values of the relevant parameters in the Rietkerk model (4a).

Empirical data on the historical origin of vegetation patterns is very limited indeed. The issue is not even mentioned in most recent literature, but it was considered by a number of the early papers in the field, from the 1950s and 1960s. That discussion does suggest colonisation as the origin of some instances of vegetation bands, which were usually termed arcs at that time. Greenwood (1957) concluded that colonisation was the cause of arc formation at a site in Somaliland (modern day north-west Somalia). This was based on the observation of small "embryo arcs" in aerial photographs, and the author presented detailed arguments on how these could develop into a full-blown pattern. White (1969) presented more quantitative evidence from a site in Jordan. He noted that the soil in the bare interbands had been highly sodic (i.e. had a high sodium content) for "some considerable time", which argues against degradation of previously uniform vegetation. However other early papers argue in favour of degradation of uniform vegetation to form bands, although with very little supportive evidence (Boaler and Hodge 1964; Hemming 1965). More recently Kusserow and Haenisch (1999)

have also drawn this conclusion, based on a comparison of aerial photographs of a single location between 1950 and 1996. Taken together, these papers suggest that colonisation of bare ground and degradation of uniform vegetation do both act as generators of vegetation patterns in the field. Definitive conclusions about pattern origin require long-term photographic records. Currently, comprehensive data of this type dates back only to the US spy satellite missions of the 1960s, with a much more limited collection of aerial photographs from the late 1940s and 1950s. As time progresses, the lengthening of this database will reveal a clearer picture of pattern origin. In the mean time one must rely on proxy data; in particular, I have shown recently that it may be possible to infer pattern origin from the relationship between the wavelength of banded vegetation and the slope gradient (Sherratt 2015).

Acknowledgments I am grateful to Eleanor Tanner for valuable discussions.

References

- Anderson KE, Hilker FM, Nisbet RM (2012) Directional biases and resource-dependence in dispersal generate spatial patterning in a consumer–producer model. *Ecol Lett* 15:209–217
- Archer NAL, Quinton JN, Hess TM (2012) Patch vegetation and water redistribution above and below ground in south-east Spain. *Ecohydrology* 5:108–120
- Atkinson K, Weimin H, Stewart DE (2009) Numerical solution of ordinary differential equations. Wiley, Hoboken
- Barbier N, Couteron P, Lejoly J, Deblauwe V, Lejeune O (2006) Self-organized vegetation patterning as a fingerprint of climate and human impact on semi-arid ecosystems. *Ecology* 94:537–547
- Baudena M, Rietkerk M (2013) Complexity and coexistence in a simple spatial model for arid savanna ecosystems. *Theor Ecol* 6:131–141
- Bel G, Hagberg A, Meron E (2012) Gradual regime shifts in spatially extended ecosystems. *Theor Ecol* 5:591–604
- Benguria RD, Depassier MC (2014) Shift in the speed of reaction–diffusion equation with a cut-off: pushed and bistable fronts. *Phys D* 280:38–43
- Berg SS, Dunkerley DL (2004) Patterned mulga near Alice Springs, central Australia, and the potential threat of firewood collection on this vegetation community. *J Arid Environ* 59:313–350
- Boaler SB, Hodge CAH (1964) Observations on vegetation arcs in the northern region, Somali Republic. *J Ecol* 52:511–544
- Bochet E, García-Fayos P, Poesen J (2009) Topographic thresholds for plant colonization on semi-arid eroded slopes. *Earth Surf Proc Land* 34:1758–1771
- Bonachela JA, Pringle RM, Sheffer E, Coverdale TC, Guyton JA, Caylor KK, Levin SA, Tarnita CE (2015) Termite mounds can increase the robustness of dryland ecosystems to climatic change. *Science* 347:651–655
- Borthagaray AI, Fuentes MA, Marquet PA (2010) Vegetation pattern formation in a fog-dependent ecosystem. *J Theor Biol* 265:18–26
- Buis E, Veldkamp A, Boeken B, Van Breemen N (2009) Controls on plant functional surface cover types along a precipitation gradient in the Negev Desert of Israel. *J Arid Environ* 73:82–90
- Cantón Y, Del Barrio G, Solé-Benet A, Lázaro R (2004) Topographic controls on the spatial distribution of ground cover in the Tabernas badlands of SE Spain. *Catena* 55:341–365
- Carteni F, Marasco A, Bonanomi G, Mazzoleni S, Rietkerk M, Giannino F (2012) Negative plant soil feedback and ring formation in clonal plants. *J Theor Biol* 313:153–161
- Caylor KK, Okin GS, Turnbull L, Wainwright J, Wiegand T, Franz TE, Parsons AJ (2014) Integrating short- and long-range processes into models: the emergence of pattern. In: Mueller EV, Wainwright J, Parsons AJ, Turnbull L (eds) *Patterns of land degradation in drylands—understanding self-organised ecogeomorphic systems*. Springer, Dordrecht, pp 141–170
- Corrado R, Cherubini AM, Pennetta C (2014) Early warning signals of desertification transitions in semiarid ecosystems. *Phys Rev E* 90:062705

- Courchamp F, Berec L, Gascoigne J (2008) Allee effects in ecology and conservation. Oxford University Press, Oxford
- Cruickshank I, Gurney WS, Veitch AR (1999) The characteristics of epidemics and invasions with thresholds. *Theor Popul Biol* 56:279–292
- Dagbovie AS, Sherratt JA (2014) Pattern selection and hysteresis in the Rietkerk model for banded vegetation in semi-arid environments. *J R Soc Interface* 11:20140465
- Davis HG, Taylor CM, Lambrinos JG, Strong DR (2004) Pollen limitation causes an Allee effect in a wind-pollinated invasive grass (*Spartina alterniflora*). *PNAS USA* 101:13804–13807
- Deblauwe V, Barbier N, Couteron P, Lejeune O, Bogaert J (2008) The global biogeography of semi-arid periodic vegetation patterns. *Glob Ecol Biogeogr* 17:715–723
- Deblauwe V, Couteron P, Lejeune O, Bogaert J, Barbier N (2011) Environmental modulation of self-organized periodic vegetation patterns in Sudan. *Ecography* 34:990–1001
- Deblauwe V, Couteron P, Bogaert J, Barbier N (2012) Determinants and dynamics of banded vegetation pattern migration in arid climates. *Ecol Monogr* 82:3–21
- Dembélé F, Picard N, Karembé M, Birnbaum P (2006) Tree vegetation patterns along a gradient of human disturbance in the Sahelian area of Mali. *J Arid Environ* 64:284–297
- Dralle D, Boisrime G, Thompson SE (2014) Spatially variable groundwater recharge and the hillslope hydrologic response: analytical solutions to the linearized hillslope Boussinesq equation. *Water Resour Res* 50:8515–8530
- Duffy KJ, Patrick KL, Johnson SD (2013) Does the likelihood of an Allee effect on plant fecundity depend on the type of pollinator? *J Ecol* 101:953–962
- Dunkerley DL, Brown KJ (2002) Oblique vegetation banding in the Australian arid zone: implications for theories of pattern evolution and maintenance. *J Arid Environ* 52:163–181
- Galle S, Ehrmann M, Peugeot C (1999) Water balance in a banded vegetation pattern: a case study of tiger bush in western Niger. *Catena* 37:197–216
- Gilad E, von Hardenberg J, Provenzale A, Shachak M, Meron E (2004) Ecosystem engineers: from pattern formation to habitat creation. *Phys Rev Lett* 93:098105
- Gilad E, Von Hardenberg J, Provenzale A, Shachak M, Meron E (2007) A mathematical model of plants as ecosystem engineers. *J Theor Biol* 244:680–691
- Gowda K, Riecke H, Silber M (2014) Transitions between patterned states in vegetation models for semiarid ecosystems. *Phys Rev E* 89:022701
- Greenwood JEGW (1957) The development of vegetation patterns in Somaliland Protectorate. *Geogr J* 123:465–473
- Gurney WSC, Veitch AR, Cruickshank I, McGeachin G (1998) Circles and spirals: population persistence in a spatially explicit predator–prey model. *Ecology* 79:2516–2530
- Guttal V, Jayaprakash C (2007) Self-organization and productivity in semi-arid ecosystems: implications of seasonality in rainfall. *J Theor Biol* 248:290–500
- Hagan PS (1981) The instability of non-monotonic wave solutions of parabolic equations. *Stud Appl Math* 64:57–88
- Hejmanová P, Hejman M, Camara AA, Antonínová M (2010) Exclusion of livestock grazing and wood collection in dryland savannah: an effect on long-term vegetation succession. *Afr J Ecol* 48:408–417
- Hemming CF (1965) Vegetation arcs in Somaliland. *J Ecol* 53:57–67
- Henry D (1981) Geometric theory of semilinear parabolic equations. Springer, Berlin
- HilleRisLambers R, Rietkerk M, van de Bosch F, Prins HHT, de Kroon H (2001) Vegetation pattern formation in semi-arid grazing systems. *Ecology* 82:50–61
- Hooper DU, Johnson L (1999) Nitrogen limitation in dryland ecosystems: responses to geographical and temporal variation in precipitation. *Biogeochemistry* 46:247–293
- Istanbuluoglu E, Bras RL (2006) On the dynamics of soil moisture, vegetation, and erosion: implications of climate variability and change. *Water Resour Res* 42:W06418
- Kealy BJ, Wollkind DJ (2012) A nonlinear stability analysis of vegetative Turing pattern formation for an interaction–diffusion plant–surface water model system in an arid flat environment. *Bull Math Biol* 74:803–833
- Kéfi S, Rietkerk M, van Baalen M, Loreau M (2007) Local facilitation, bistability and transitions in arid ecosystems. *Theor Popul Biol* 71:367–379
- Kéfi S, Rietkerk M, Katul GG (2008) Vegetation pattern shift as a result of rising atmospheric CO₂ in arid ecosystems. *Theor Popul Biol* 74:332–344
- Klausmeier CA (1999) Regular and irregular patterns in semiarid vegetation. *Science* 284:1826–1828

- Kletter AY, von Hardenberg J, Meron E, Provenzale A (2009) Patterned vegetation and rainfall intermittency. *J Theor Biol* 256:574–583
- Kusserow H, Haenisch H (1999) Monitoring the dynamics of “tiger bush” (brousse tigrée) in the West African Sahel (Niger) by a combination of Landsat MSS and TM, SPOT, aerial and kite photographs. *Photogramm Fernerkund Geoinf* 2:77–94
- Lefever R, Lejeune O (1997) On the origin of tiger bush. *Bull Math Biol* 59:263–294
- Lefever R, Barbier H, Couteron P, Lejeune O (2009) Deeply gapped vegetation patterns: on crown/root allometry, criticality and desertification. *J Theor Biol* 261:194–209
- Liu Q-X, Jin Z, Li BL (2008) Numerical investigation of spatial pattern in a vegetation model with feedback function. *J Theor Biol* 254:350–360
- Marasco A, Iuorio A, Carteni F, Bonanomi G, Tartakovsky DM, Mazzoleni S, Giannino F (2014) Vegetation pattern formation due to interactions between water availability and toxicity in plant-soil feedback. *Bull Math Biol* 76:2866–2883
- Martínez-García R, Calabrese JM, García EH, López C (2014) Minimal mechanisms for vegetation patterns in semiarid regions. *Philos Trans R Soc A* 372:20140068
- Meron E (2012) Pattern-formation approach to modelling spatially extended ecosystems. *Ecol Model* 234:70–82
- Meron E, Gilad E, von Hardenberg J, Shachak M, Zarmi Y (2004) Vegetation patterns along a rainfall gradient. *Chaos Solitons Fractals* 19:367–376
- Moreno-de las Heras M, Saco PM, Willgoose GR, Tongway DJ (2012) Variations in hydrological connectivity of Australian semiarid landscapes indicate abrupt changes in rainfall-use efficiency of vegetation. *J Geophys Res* 117:G03009
- Müller J (2013) Floristic and structural pattern and current distribution of tiger bush vegetation in Burkina Faso (West Africa), assessed by means of belt transects and spatial analysis. *Appl Ecol Environ Res* 11:153–171
- Murray JD (2003) *Mathematical biology II: spatial models and biomedical applications*. Springer, New York
- Nippert JB, Knapp AK (2007a) Soil water partitioning contributes to species coexistence in tallgrass prairie. *Oikos* 116:1017–1029
- Nippert JB, Knapp AK (2007b) Linking water uptake with rooting patterns in grassland species. *Oecologia* 153:261–272
- Penny GG, Daniels KE, Thompson SE (2013) Local properties of patterned vegetation: quantifying endogenous and exogenous effects. *Philos Trans R Soc A* 371:20120359
- Pelletier JD, DeLong SB, Orem CA, Becerra P, Compton K, Gressett K, Lyons-Baral J, McGuire LA, Molaro JL, Spinler JC (2012) How do vegetation bands form in dry lands? Insights from numerical modeling and field studies in southern Nevada, USA. *J Geophys Res* 117:F04026
- Popović N (2011) A geometric analysis of front propagation in a family of degenerate reaction–diffusion equations with cutoff. *ZAMM* 62:405–437
- Pueyo Y, Kéfi S, Alados CL, Rietkerk M (2008) Dispersal strategies and spatial organization of vegetation in arid ecosystems. *Oikos* 117:1522–1532
- Pueyo Y, Moret-Fernández D, Saiz H, Bueno CG, Alados CL (2013) Relationships between plant spatial patterns, water infiltration capacity, and plant community composition in semi-arid mediterranean ecosystems along stress gradients. *Ecosystems* 16:452–466
- Rietkerk M, Ketner P, Burger J, Hoorens B, Olf H (2000) Multiscale soil and vegetation patchiness along a gradient of herbivore impact in a semi-arid grazing system in West Africa. *Plant Ecol* 148:207–224
- Rietkerk M, Boerlijst MC, van Langevelde F, HilleRisLambers R, van de Koppel J, Prins HHT, de Roos A (2002) Self-organisation of vegetation in arid ecosystems. *Am Nat* 160:524–530
- Rietkerk M, Dekker SC, de Ruiter PC, van de Koppel J (2004) Self-organized patchiness and catastrophic shifts in ecosystems. *Science* 305:1926–1929
- Saco PM, Willgoose GR, Hancock GR (2007) Eco-geomorphology of banded vegetation patterns in arid and semi-arid regions. *Hydrol Earth Syst Sci* 11:1717–1730
- Schwinning S (2010) The ecohydrology of roots in rocks. *Ecohydrology* 3:238–245
- Sheffer E, Hardenberg J, Yizhaq H, Shachak M, Meron E (2013) Emerged or imposed: a theory on the role of physical templates and self-organisation for vegetation patchiness. *Ecol Lett* 16:127–139
- Sherratt JA (2005) An analysis of vegetation stripe formation in semi-arid landscapes. *J Math Biol* 51:183–197

- Sherratt JA (2010) Pattern solutions of the Klausmeier model for banded vegetation in semi-arid environments I. *Nonlinearity* 23:2657–2675
- Sherratt JA (2011) Pattern solutions of the Klausmeier model for banded vegetation in semi-arid environments II. Patterns with the largest possible propagation speeds. *Proc R Soc Lond A* 467:3272–3294
- Sherratt JA (2013a) History-dependent patterns of whole ecosystems. *Ecol Complex* 14:8–20
- Sherratt JA (2013b) Pattern solutions of the Klausmeier model for banded vegetation in semi-arid environments III: the transition between homoclinic solutions. *Phys D* 242:30–41
- Sherratt JA (2013c) Pattern solutions of the Klausmeier model for banded vegetation semi-arid environments IV: slowly moving patterns and their stability. *SIAM J Appl Math* 73:330–350
- Sherratt JA (2013d) Pattern solutions of the Klausmeier model for banded vegetation in semi-arid environments V: the transition from patterns to desert. *SIAM J Appl Math* 73:1347–1367
- Sherratt JA (2015) Using wavelength and slope to infer the historical origin of semi-arid vegetation bands. *PNAS USA* 112:4202–4207
- Sherratt JA, Lord GJ (2007) Nonlinear dynamics and pattern bifurcations in a model for vegetation stripes in semi-arid environments. *Theor Popul Biol* 71:1–11
- Sherratt JA, Synodinos AD (2012) Vegetation patterns and desertification waves in semi-arid environments: mathematical models based on local facilitation in plants. *Discret Contin Dyn Syst Ser B* 17:2815–2827
- Sherratt JA, Smith MJ, Rademacher JDM (2010) Patterns of sources and sinks in the complex Ginzburg–Landau equation with zero linear dispersion. *SIAM J Appl Dyn Syst* 9:883–918
- Siero E, Doelman A, Eppinga MB, Rademacher J, Rietkerk M, Siteur K (2015) Stripe pattern selection by advective reaction–diffusion systems: resilience of banded vegetation on slopes. *Chaos* 25:036411
- Siteur K, Eppinga MB, Karssenben D, Baudena M, Bierkens MFP, Rietkerk M (2014a) How will increases in rainfall intensity affect semiarid ecosystems? *Water Resour Res* 50:5980–6001
- Siteur K, Siero E, Eppinga MB, Rademacher J, Doelman A, Rietkerk M (2014b) Beyond Turing: the response of patterned ecosystems to environmental change. *Ecol Complex* 20:81–96
- Stewart J, Parsons AJ, Wainwright J, Okin GS, Bestelmeyer B, Fredrickson EL, Schlesinger WH (2014) Modelling emergent patterns of dynamic desert ecosystems. *Ecol Monogr* 84:373–410
- Thompson S, Katul G (2009) Secondary seed dispersal and its role in landscape organization. *Geophys Res Lett* 36:L02402
- Thompson SE, Harman CJ, Heine P, Katul GG (2010) Vegetation–infiltration relationships across climatic and soil type gradients. *J Geophys Res Biogeosci* 115:G02023
- Thompson S, Katul G, Konings A, Ridolfi L (2011) Unsteady overland flow on flat surfaces induced by spatial permeability contrasts. *Adv Water Res* 34:1049–1058
- Tongway DJ, Ludwig JA (2001) Theories on the origins, maintenance, dynamics, and functioning of banded landscapes. In: Tongway DJ, Valentin C, Seghier J (eds) *Banded vegetation patterning in arid and semi-arid environments*. Springer, New York, pp 20–31
- Ursino N (2005) The influence of soil properties on the formation of unstable vegetation patterns on hillsides of semiarid catchments. *Adv Water Resour* 28:956–963
- Ursino N, Contarini S (2006) Stability of banded vegetation patterns under seasonal rainfall and limited soil moisture storage capacity. *Adv Water Resour* 29:1556–1564
- Valentin C, d'Herbès JM, Poesen J (1999) Soil and water components of banded vegetation patterns. *Catena* 37:1–24
- van der Stelt S, Doelman A, Hek G, Rademacher JDM (2013) Rise and fall of periodic patterns for a generalized Klausmeier–Gray–Scott model. *J Nonlinear Sci* 23:39–95
- Vezzoli R, De Michele C, Pavlopoulos H, Scholes RJ (2008) Dryland ecosystems: the coupled stochastic dynamics of soil water and vegetation and the role of rainfall seasonality. *Phys Rev E* 77:051908
- von Hardenberg J, Meron E, Shachak M, Zarmi Y (2001) Diversity of vegetation patterns and desertification. *Phys Rev Lett* 87:198101
- White LP (1969) Vegetation arcs in Jordan. *J Ecol* 57:461–464
- Worrall GA (1959) The Butana grass patterns. *J Soil Sci* 10:34–53
- Wu XB, Thurow TL, Whisenant SG (2000) Fragmentation and changes in hydrologic function of tiger bush landscapes, south-west Niger. *J Ecol* 88:790–800
- Yizhaq H, Sela S, Svoray T, Assouline S, Bel G (2014) Effects of heterogeneous soil-water diffusivity on vegetation pattern formation. *Water Resour Res* 50:5743–5758
- Zelnik YR, Kinast S, Yizhaq H, Bel G, Meron E (2013) Regime shifts in models of dryland vegetation. *Philos Trans R Soc A* 371:20120358